Immunity
Article

The Sensing of Environmental Stimuli by Follicular Dendritic Cells Promotes Immunoglobulin A Generation in the Gut

Keiichiro Suzuki,[1] Mikako Maruya,[1] Shimpei Kawamoto,[1,3] Katarzyna Sitnik,[4] Hiroshi Kitamura,[2] William W. Agace,[4] and Sidonia Fagarasan[1,*]
[1]Laboratory for Mucosal Immunity
[2]Laboratory for Immunogenomics
Research Center for Allergy and Immunology, RIKEN Yokohama 1-7-22, Tsurumi, Yokohama, 230-0045, Japan
[3]Department of Immunology and Genomic Medicine, Kyoto University, Graduate School of Medicine, Sakyo-ku, Kyoto 606-8501, Japan
[4]Section for Immunology, Lund University, Lund 221 84, Sweden
*Correspondence: sidonia-f@rcai.riken.jp
DOI 10.1016/j.immuni.2010.07.003

SUMMARY

In the Peyer's patches (PPs), germinal centers (GCs) are chronically induced by bacteria and are the major sites for generation of gut immunoglobulin A (IgA) immune responses. Whether follicular dendritic cells (FDCs) within the GCs directly contribute to the IgA production in PPs is unknown. We showed here that direct stimulation of FDCs by bacterial products and retinoic acid synergistically enhanced the expression of the chemokine CXCL13, the survival factor BAFF, and molecules that facilitate the secretion and activation of the cytokine TGF-β1. A reduced production of these molecules by PP FDCs associated with deficiencies in the Toll-like receptor pathway or vitamin A resulted in decreased numbers of GC B cells and defective generation of IgA$^+$ B cells within PP GCs. Our data indicate that PP FDCs are conditioned by environmental stimuli to express key factors for B cell migration, survival, and preferential generation of IgA in gut.

INTRODUCTION

Immune responses to antigens occur predominantly in organized lymphoid structures such as Peyer's patches (PPs) and lymph nodes (LNs). These structures contain hematopoietic cells strategically segregated into B cell and T cell areas, with each area built on and functionally influenced by different types of nonhematopoietic cells, generally called stromal cells (SCs) (Allen and Cyster, 2008). Thus, B cells cluster and form follicles around SCs known as follicular dendritic cells (FDCs) expressing CXCL13 chemokine, whereas T cells, together with dendritic cells (DCs), locate adjacent to B cell follicles in a reticular network composed of fibroblastic reticular cells (FRCs) producing CCL19 and CCL21 chemokines (Allen and Cyster, 2008; Katakai et al., 2004; Luther et al., 2000). Upon antigenic stimulation, both lymphocyte and SC compartments respond and undergo extensive remodeling. For example, during T cell-dependent immune responses, the FRC network expands to facilitate T cell accumulation and their activation upon cognate interaction with antigen-presenting cells (i.e., DCs) (Katakai et al., 2004). In parallel, within the B cell area, FDCs undergo phenotypic maturation by increasing expression of adhesion molecules (VCAM-1, ICAM-1, MadCAM-1) and low-affinity Fc receptors (CD23, also known as FcεRII and CD32, also known as FcγRIIb) and by deposition of immune complexes, resulting in germinal center (GC) development (Allen and Cyster, 2008).

GCs are unique microarchitectural units within B cell follicles, where antigen-specific B cells proliferate, upregulate activation-induced cytidine deaminase (AID), and undergo class-switch recombination and somatic mutations (Muramatsu et al., 2000). These two AID-dependent genetic alterations, as well as affinity selection, possibly by immune complexes displayed on FDCs, allow generation of memory B cells and plasmablasts, whose antibodies bind to the eliciting antigen with a high affinity.

Several characteristics distinguish GCs in gut PPs from GCs in peripheral LNs (pLNs) (Suzuki and Fagarasan, 2008). For instance, GCs are always detected in PPs, as they are induced under constant stimulation by commensal bacteria. Indeed, animals kept in germ-free conditions or those treated with antibiotics that eliminate the indigenous flora have extremely few GCs in PPs (Fagarasan et al., 2002). By contrast, GCs in pLNs develop only upon systemic infections or after deliberate immunization. Furthermore, GCs can be induced in PPs and gut-draining mesenteric LNs (mLNs), but not in pLNs, in the absence of antigen-specific recognition through the B cell receptors. This induction occurs when B cells are activated by bacterial antigens through innate receptors, such as Toll-like receptors (TLRs), with T cell help (Casola et al., 2004). Indeed, T cells located within the B cell follicles, called follicular B helper T (Tfh) cells, play key roles in GC reactions (King et al., 2008).

PP GCs also differ from pLN GCs in regard to the isotype and the amount of antibodies produced. Thus, B cells in mucosal GCs undergo preferential class switching to IgA, whereas activated B cells located in pLN GCs generate predominantly IgG antibodies. IgAs secreted into the gut lumen join innate immune defenses and provide protection by preventing bacterial

attachment to the gut epithelium and by regulating bacterial communities in the gut (Fagarasan et al., 2002; Peterson et al., 2007; Suzuki et al., 2004).

The molecular and cellular mechanisms underlying the continuous presence of GCs in PPs and the almost exclusive generation of IgA in mucosal GCs are incompletely understood, but probably involve signals provided both by cellular components of GCs and by environmental factors. For example, FDCs are critical for enhancing the proliferation and differentiation of activated B cells and for the maintenance of GCs (Grouard et al., 1995; Wu et al., 2008). In turn, GC B cells contribute to maturation and maintenance of FDCs by providing LTα1β2 (Allen and Cyster, 2008; Gommerman and Browning, 2003). The predominance of IgA class switching in the gut is explained by (1) the constant bacterial pressure on B cells, which facilitate sequential transcription of the IgH constant region from Cμ to Cα and (2) the unique metabolic products and cytokine milieu produced by activated B cells, DCs, T cells, and epithelial cells (IL-6, IL-10, IL-21, TGF-β1, retinoic acid [RA], the active metabolite of vitamin A [VA]) (Cerutti and Rescigno, 2008; Suzuki and Fagarasan, 2008). However, whether FDCs contribute to IgA production in PP GCs is unknown. Furthermore, if FDCs recognize specific gut stimuli and whether they modulate their function in response to the local environment has not been addressed. This is an important issue because within the GCs, lymphocytes and FDCs are in a continuous dialog, and any changes in one compartment would likely trigger modifications in the other compartment, leading to functional modifications by multiple feedback and forward mechanisms.

Here, we demonstrate that FDCs are equipped with surface, cytoplasmic, and nuclear receptors that signaled the presence of bacterial and metabolic products such as RA. In vivo and in vitro response of FDCs to stimulation through TLR and RA receptors (RARs) resulted in the upregulation of chemokines, survival factors, and molecules involved in the activation of TGF-β1, an anti-inflammatory cytokine essential for IgA class switching. Our data indicate that gut FDCs are conditioned by environmental stimuli to express key factors required to sustain the GC reaction and to facilitate preferential generation of IgA within mucosal GCs.

RESULTS

FDCs Express TLRs and RARs

PP FDCs and pLN FDCs were isolated by a technique that combines tissue digestion, magnetic bead enrichment, and flow cytometry sorting based on high expression of FDC-M1 (an antigen identified as milk fat globule epidermal growth factor 8, Mfge8) and CD21 and CD35 (Kranich et al., 2008; Sukumar et al., 2006) (Figure 1A). This method, although probably precluding the isolation of some FDCs expressing low FDC-M1 from the pLNs of nonimmunized mice (Allen and Cyster, 2008), allowed a good separation of FDCs from other cells expressing FDC-M1 (i.e., tingible body macrophages) (Figure S1A). Purified cells expressed high FDC-associated transcripts (i.e., Mfge8, clusterin, and prion protein) and had typical features of FDCs: they were large cells, with multiple and round-shaped big nuclei and abundant, granular cytoplasm (Grouard et al., 1995; Huber et al., 2005; Sukumar et al., 2006) (Figures 1B and S1B). In addition to FDC-M1 and complement receptors CD21 and CD35, these cells expressed surface molecules involved in GC biology, such as FcγRII and FcγRIII, ICAM-1, VCAM-1, and LTβR, and could be cultured in vitro for more than 1 week in the presence of TNF-α and agonist antibody for LTβR, two essential factors required for maintenance of FDCs (Nishikawa et al., 2006) (Figure 1C and data not shown).

A previous study indicated that pLN FDCs express TLR4 and that engagement of TLR4 by LPS upregulates FcγRIIB, VCAM-1, and ICAM-1 expression and promotes accessory activity of FDCs (El Shikh et al., 2007). Thus, we investigated whether FDCs express other receptors capable of recognizing bacterial and food-derived components present in the gut environment. We found that most of the TLR transcripts were not only expressed, but highly enriched on FDCs (Figure S1C). PP FDCs expressed lower mRNA and had reduced intracellular and surface TLR2 and TLR4 compared with pLN FDCs (Figures 1C, S1C, and S1D). The downregulation of TLRs by PP FDCs may reflect the engagement of these receptors by their ligands, the presence of high amounts of RA, or both (Liu et al., 2005; Nomura et al., 2000). Indeed, in addition to TLRs, FDCs expressed transcripts for RARs (Figure 1D). The expression of RARα and RARγ transcripts was slightly higher in pLN than in PP FDCs, and these receptors, especially RARγ, were abundantly expressed also by other cells present in pLNs. By contrast, RARβ transcripts were abundantly and predominantly expressed by PP FDCs as compared with pLN FDCs or with whole-tissue preparations. The expression of RARβ in FDCs prepared from mLNs was intermediate between that of FDCs isolated from PPs and pLNs. The higher RARβ expression in mucosal-derived FDCs than in pLN FDCs likely reflects high amounts of RA present locally, because (1) RARβ expression was reduced and equally low in PP, mLN, and pLN FDCs isolated from mice kept on VA-deficient diet (VAD mice) and (2) stimulation of pLN FDCs with RA (but not with several microbial components) considerably induced the RARβ expression (Figures 1E and 1F).

RARs regulate gene expression by binding to RA-responsive elements (RAREs) (Germain et al., 2006). To directly determine whether FDCs receive RA signals in vivo, pLN, mLN, and PP FDCs were isolated from DR5-luciferase RARE reporter mice (Svensson et al., 2008). We found constitutive luciferase expression (RA signaling) to be higher in PP FDCs than in pLN FDCs (Figure 1G). As with RARβ expression, amounts of luciferase in mLN FDCs were intermediate between that of PP and pLN FDCs.

PP FDCs have clear fingerprints of RA signaling, but they do not appear to convert VA into active retinoid metabolites. The expression of RA-producing enzymes (ADHs and RALDHs) was very low in ex vivo FDCs and further decreased in these cells after in vitro culturing (Figure S1E). Interestingly, abundant expression of RALDH1 was detected in whole PP preparations, but this was confirmed at the protein level to be mainly produced by the epithelial cells, as previously proposed (Iwata et al., 2004).

We conclude that FDCs are equipped with surface, cytoplasmic, and nuclear receptors that are activated by microbial products and metabolites of VA.

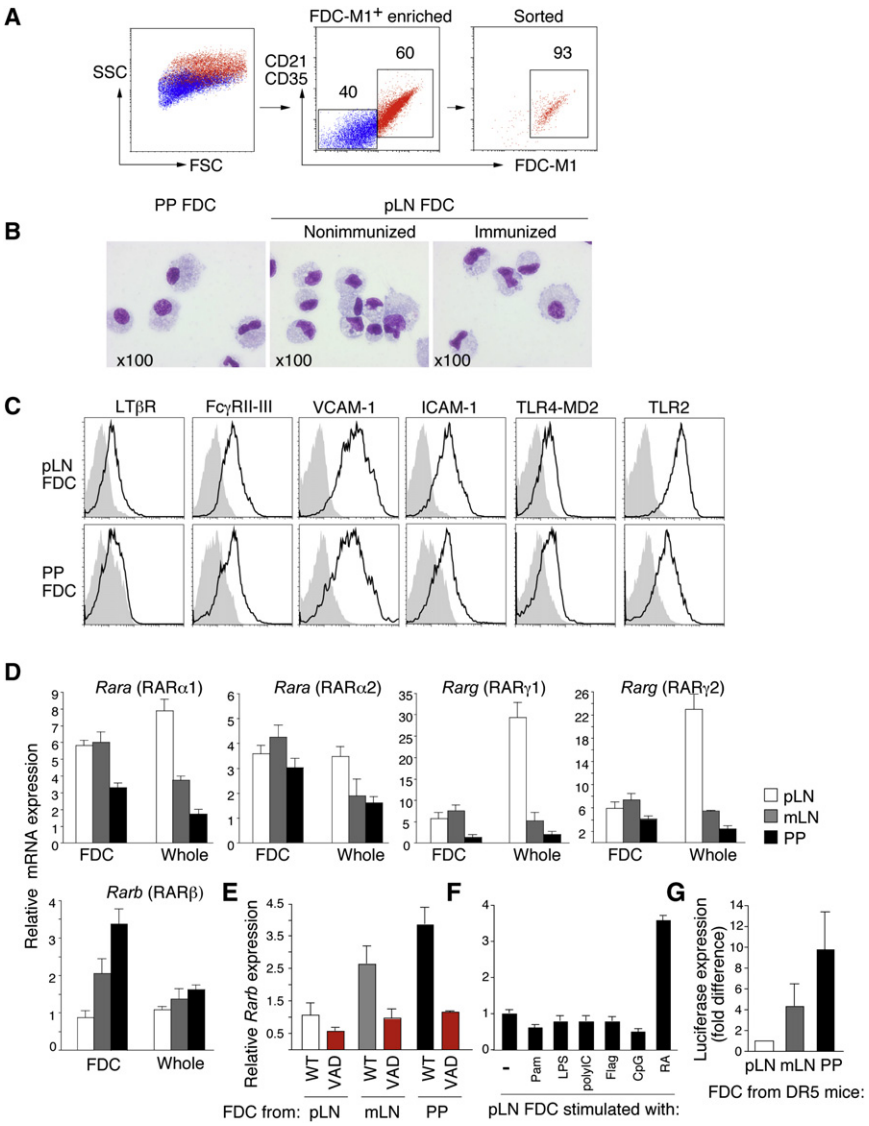

Figure 1. Isolation and Characterization of FDCs from PPs and pLNs

(A) Representative flow cytometric profiles of magnetically enriched (left and middle panels) and flow cytometry-purified (right panel) FDCs, stained for FDC-M1 and CD21 or CD35. Red and blue colored dots represent FDC-M1^{hi}CD21 or CD35^{+} cells and FDC-M1^{lo}CD21 or CD35^{-} cells, respectively. Numbers on plots indicate the frequency of cells in the gate.

(B) May-Grünwald-Giemsa staining of flow cytometry-purified FDCs isolated from PPs and pLNs before and after immunization with TNP-KLH.

(C) Flow cytometry for the indicated molecules on the surface of FDC-M1^{hi} cells isolated from PPs and pLNs. Shaded histograms represent isotype control antibodies. Data are representative of three independent experiments.

(D) Q-PCR analyses of indicated *Rar* gene expression, relative to housekeeping gene *Gapdh*, in freshly purified FDCs and whole tissues of the indicated organs.

(E and F) Q-PCR analyses of *Rarb* expression in FDCs freshly isolated from the PPs, mLNs, and pLNs of WT mice and VAD mice (E) and FDCs purified from pLNs and cultured for 4 days with an agonist LTβR antibody and TNF-α, without or with the indicated stimuli (F). Data are representative of at least three experiments (mean ±SEM).

(G) Q-PCR analyses of luciferase expression (relative to β-actin) in FDCs from PPs, mLNs, and pLNs of DR5-luciferase RARE reporter mice. pLN FDC expression was set as 1; n = 8–10 mice/experiment; data are from two experiments (mean ±SEM).

Unique Characteristics of GC FDCs in PPs

To investigate if PP FDCs have different characteristics from pLN FDCs, we first compared their gene expression profiles. We found that ~92% of the gene transcripts expressed by FDCs were shared between PP and pLN FDCs. Nevertheless, a number of transcripts (about 2000 of the 11,313 genes expressed) were overrepresented either in PP FDCs or in the pLN FDCs (Figure 2A). However, these differences could be easily attributed to different activation or maturation status of the FDCs (Allen and Cyster, 2008). To eliminate this possibility, we immunized mice with trinitrophenol-keyhole limpet hemocyanin (TNP-KLH) together with incomplete Freund's adjuvant (IFA). One week after immunization, the percentage of GC B cells in pLNs was similar to that in PPs, and the majority of FDCs were GC FDCs, located in secondary follicles containing AID-expressing B cells (Figure 2B and data not shown). Surprisingly, many genes were downregulated after maturation of pLN FDCs induced upon immunization, as indicated by the subtle but clear off-diagonal shift of the transcripts of FDCs from nonimmunized pLNs. In contrast, the differences observed between PP and immunized pLN FDC transcripts were not only maintained, but even enhanced (Figure 2A). The profile of pLN FDCs remained different from that of PP FDCs even after immunization with TNP-KLH in the presence of more innate stimuli. Indeed, only about 14% of the genes induced after immunization with TNP-KLH in complete Freund's adjuvant (CFA) without or with a TLR2-TLR6 ligand (Pam2CSK4) overlapped with those highly expressed by the PP FDCs (Figure S2).

Among the genes overexpressed in PP FDCs were those for molecules involved in lymphocyte recruitment and retention (CXCL13, MadCAM-1, collagens), survival factors (BAFF, clusterin), and molecules associated with secretion and activation of TGF-β1, herein called TGF-β activators (CD36, latent TGF-β binding proteins [LTBP1, LTBP2, LTBP3], matrix metalloproteinases [MMP2, MMP9], bone morphogenic protein [BMP2], integrin αv subunit) (Figure 2C). Quantitative PCR analyses confirmed the differences in gene expression between PP FDCs and pLN FDCs (Figure 2D and data not shown).

Thus, FDCs located in PP GCs have features distinctive from FDCs present in GCs of pLNs.

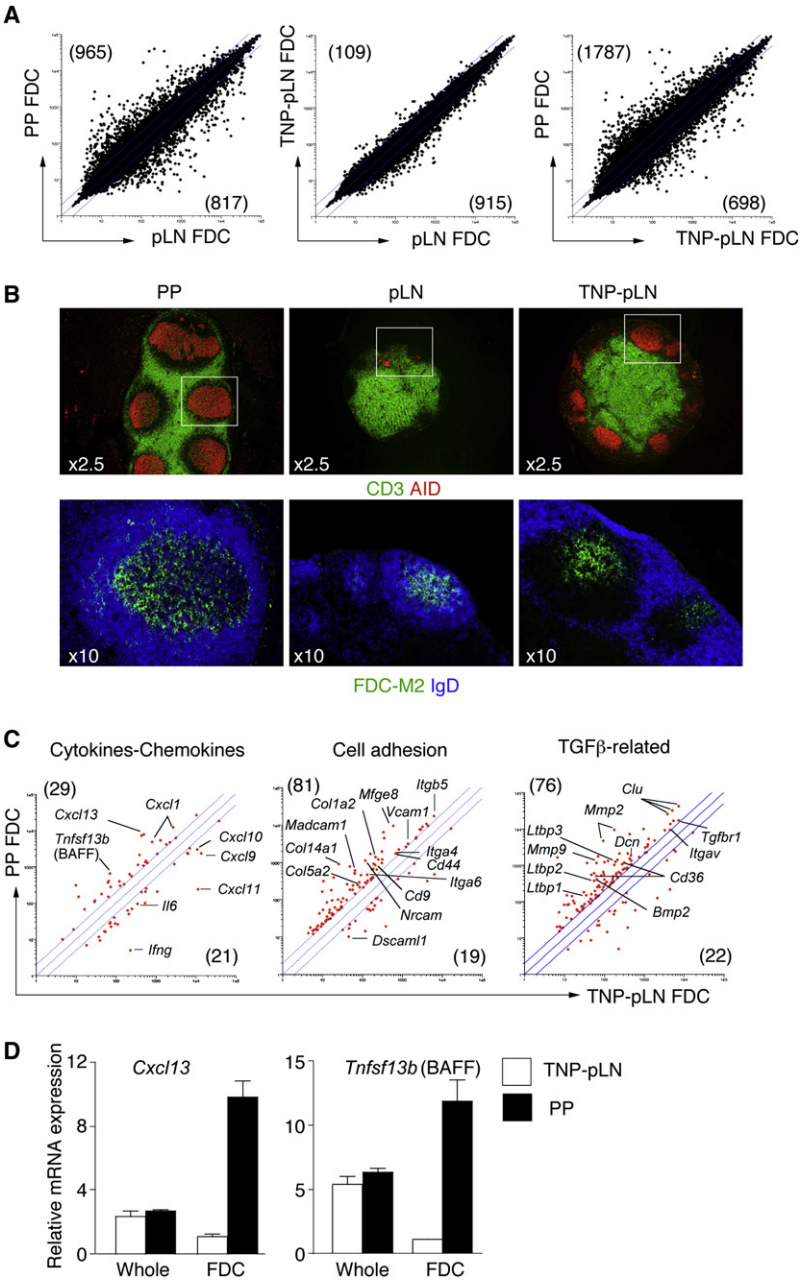

Figure 2. PP FDCs Express More Abundant Transcripts for Adhesion Molecules, Chemokines, and TGF-β1 Activators Than FDCs from pLNs

(A) Comparison of probe-expression values in ex vivo FDCs isolated from PPs (y axis) and pLNs (x axis) without immunization (left panel), from pLNs without immunization (x axis) and pLNs after immunization with TNP-KLH in IFA (y axis) (middle panel), and from PPs (y axis) and pLNs after immunization with TNP-KLH in IFA (x axis) (right panel). The number of transcripts that have differential levels of expression (cut off; 2-fold) is shown in the parenthesis. Each dot represents the mean of normalized expression level from 2 (TNP-pLN FDC) or 3 (pLN and PP FDCs) independent experiments. All the profiling was done with flow cytometry-sorted FDC-M1^{hi}CD21 or CD35^{+} cells pooled from 10–20 mice.

(B) Immunofluorescent microscopy analysis of AID and CD3 staining and FDC-M2 and IgD staining in sections of PP, naive pLN, and pLN after immunization with TNP-KLH in IFA.

(C) Genes encoding cytokines, chemokines, and adhesion molecules were selected according to the annotation data in the RefDIC tools (http://refdic.rcai.riken.jp/tools.cgi). Molecules related with TGF-β1 were extracted based on the GeneCards program (http://www.genecards.org/index.shtml). Dots represent probes expressed more in PP FDCs or pLN FDCs after immunization with TNP-KLH in IFA (cut off: 2-fold; the number of probes is shown in parenthesis).

(D) Q-PCR analyses showing expression of *Cxcl13* and *Tnfsf13b* (BAFF) relative to housekeeping gene *Gapdh* by freshly purified FDCs and by whole tissues of indicated organs. TNP-pLN FDC expression was set as 1. Data are from 7–10 experiments (mean ±SEM).

pLN FDCs Acquire PP FDC Characteristics upon Stimulation through TLRs and RARs

We reasoned that GC FDCs from PPs have different features than GC FDCs from pLNs, because they are activated by different environmental stimuli. To test this hypothesis, we tried to reconstitute the PP FDC signature in vitro by pulsed or continuous stimulation of pLN FDCs through TLRs, through RARs, or simultaneously through TLRs and RARs. More than 900 transcripts were upregulated after 5 hr stimulation with LPS, but only about 20% of these transcripts overlapped with those highly expressed by PP FDCs (Figure 3A). By contrast, although the number of transcripts induced after prolonged stimulation with LPS (72 hr) or Pam2CSK4 (96 hr) was reduced compared with those induced by acute LPS stimulation, there was a notable shift in gene expression, with about 30% of the upregulated transcripts overlapping with those highly expressed ex vivo by the PP FDCs (Figures 3A and 3B). The shift toward PP FDC signature was even more pronounced after 96 hr stimulation of pLN FDCs with RA. Indeed, almost 50% of the RA-induced transcripts overlapped with those highly expressed by PP FDCs (Figure 3A). In general, the genes induced by RA stimulation did not overlap completely with those induced by stimulation through TLRs (Figure 3B). Yet stimulation with RA and TLR ligands (LPS, Pam2CSK4, or Pam3CSK4 [a TLR2-TLR1 ligand]) had a synergistic effect and enhanced the transcription of genes, such as *Cxcl13*, *Cxcl1*, *Tnfsf13b* (BAFF), *Mmp2*, and *Mmp9*, that were also highly expressed by PP FDCs (Figure 3C). Interestingly, although stimulation with RA and LPS preferentially induced *Tnfsf13b* (BAFF) expression, stimulation with RA together with Pam2CSK4 or Pam3CSK4 mostly enhanced *Cxcl13* and *Mmp*s expression (Figure S3B). However, the expression of many transcripts overrepresented in PP FDCs could not be induced in vitro by any of these stimulations (Figures 3B and S3A), indicating that perhaps other microbial or metabolic products contribute to the induction of PP FDC signature. Alternatively, and not mutually exclusive,

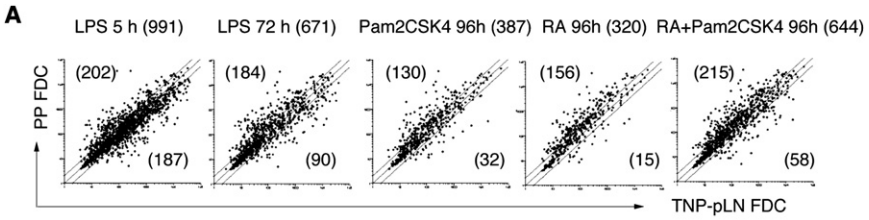

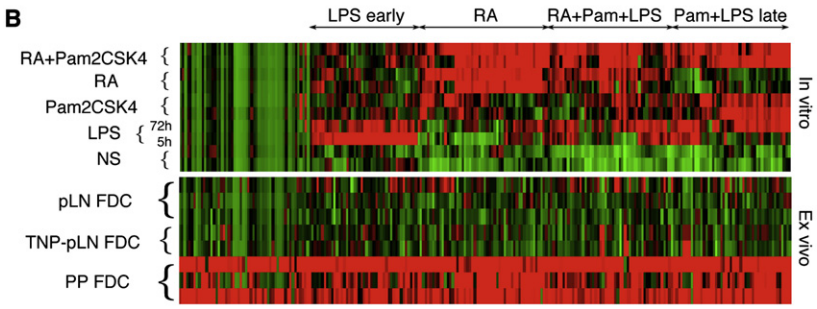

C

Symbol	Gene title	Fold change		
		Pam/NS	RA/NS	RA+Pam/NS
Cxcl13	chemokine (C-X-C motif) ligand 13	21.3	1.7	54.8
Cxcl1	chemokine (C-X-C motif) ligand 1	14.0	3.0	29.9
Mt2	metallothionein 2	3.5	3.1	20.7
Mmp2	matrix metallopeptidase 2	4.9	5.8	15.4
Mmp9	matrix metallopeptidase 9	5.4	5.7	12.3
Col5a2	collagen, type V, alpha 2	8.7	8.0	10.7
Lum	lumican	2.9	1.1	9.3
Igfbp4	insulin-like growth factor binding protein 4	3.9	11.2	9.2
Cxcl14	chemokine (C-X-C motif) ligand 14	1.3	8.6	9.1
Tnfsf13b	tumor necrosis factor (ligand) superfamily, member 13b	3.2	1.3	8.2
Cysltr1	cysteinyl leukotriene receptor 1	5.8	7.5	7.2
Serpine1	serine (or cysteine) peptidase inhibitor, clade E, member 1	4.6	4.5	6.8
Tagln	transgelin	5.1	8.6	6.5
Ltbp3	latent transforming growth factor beta binding protein 3	1.2	6.4	5.0
Ctgf	connective tissue growth factor	4.3	4.8	4.7
Fabp1	fatty acid binding protein 1, liver	2.1	1.0	4.7
Bmp2	bone morphogenetic protein 2	1.7	10.6	4.7
Smad1	MAD homolog 1 (Drosophila)	2.0	2.3	3.3
Clu	clusterin	1.3	3.5	3.3
Col1a2	collagen, type I, alpha 2	4.1	1.6	3.3
Dcn	decorin	2.7	1.3	2.9
Sparc	secreted acidic cysteine rich glycoprotein	2.3	2.7	2.4
Ltbp1	latent transforming growth factor beta binding protein 1	1.0	1.0	2.1
Ltbp2	latent transforming growth factor beta binding protein 2	2.2	2.1	1.9

Figure 3. Stimulation of pLN FDCs with RA and TLR Ligands Induces the Expression of Genes Characteristic for PP FDCs

(A) Magnetically enriched pLN FDCs were cultured without or with LPS, Pam2CSK4, or/and RA for the indicated time and then processed for microarray analysis. The genes upregulated upon stimulation (cut off; 3-fold) were selected and replotted on the panel showing probe-expression values of ex vivo FDCs purified from PPs and pLNs after immunization. The numbers of induced probes are shown at the top of each panel. The numbers shown in panels indicate the number of probes differentially expressed (cut off; 2-fold) by PP FDCs and pLN FDCs after immunization with TNP-KLH in IFA.

(B) Heat-map analysis for the PP FDC genomic signature in ex vivo PP and pLN FDCs or in vitro pLN FDCs stimulated as described in (A). See Experimental Procedures for probe selection criteria. Each row represents an independent experiment. Upregulated and downregulated transcripts are indicated in red and green, respectively.

(C) Immunologically relevant genes (cytokines and chemokines, cell adhesion molecules, TGF-β activators, and molecules with anti-inflammatory properties) were selected from the probe sets presented in (B) and arranged by fold change after Pam2CSK4 and RA stimulation.

FDCs may have undergone some changes in vitro that do not perfectly overlap with their in vivo response.

Taken together, the results strongly suggest that PP FDC signature is acquired through sustained stimulation with bacterial and food-derived components.

Reduced Expression of CXCL13 and BAFF by PP FDCs in the Absence of MyD88 and VA

To evaluate in vivo the effect of environmental factors such as bacteria and VA on PP FDCs, we performed experiments with WT, *Myd88*$^{-/-}$, and VAD mice. MyD88 is a TLR signaling adaptor downstream of most of the TLRs (Takeda and Akira, 2004). The FDC network could be easily detected, although area of FDC-M2^{+} cells and the total numbers of PP FDCs were reduced in the absence of MyD88 signaling and VA (Figures 4A, 4B, and S4D). The expression of CXCL13 and BAFF was severely reduced in FDC areas of PPs in *Myd88*$^{-/-}$ and VAD mice compared with those from WT mice (Figure 4A). Furthermore, the percentages and numbers of GC B cells as well as the size of AID-expressing B cell clusters were significantly reduced in PPs of *Myd88*$^{-/-}$ and VAD mice compared with WT mice (Figures 4C and S4). As expected, these quantitative and qualitative changes of GCs in PPs had a considerable impact on IgA production in gut: the B220^{+}IgA^{+} B cells in PPs and the B220^{-}IgA^{+} plasma cells in the small intestine LP were severely reduced in *Myd88*$^{-/-}$ mice and VAD mice as compared with WT mice (Figures 4C and S4A).

We next wanted to clarify if the impaired GC formation and IgA generation observed in the absence of TLR and RAR signaling was due to impaired activation of FDCs or of the lymphocyte compartment. To assess more directly the effect of TLR-MyD88 signaling in FDCs, we performed bone marrow (BM) transfer experiments. Thus, lethally irradiated *Myd88*$^{-/-}$ mice or WT mice were transplanted with BM cells from WT mice. In these chimeric mice, the radio-resistant FDCs were host derived, whereas all lymphocytes were derived from normal BM cells. (For obvious reasons, similar BM reconstitution experiments could not be performed with VAD mice.) The expression of CXCL13 and BAFF by PP FDCs was considerably reduced in *Myd88*$^{-/-}$ recipient mice compared with WT reconstituted mice (Figure 4D). Importantly, the numbers of both GC B cells and IgA^{+} B cells in PPs were reduced in *Myd88*$^{-/-}$ mice compared with control WT mice (Figure 4C). The number of IgA plasma cells in LP was also reduced in the absence of MyD88 in non-BM compartment, but this may be also due to a defective production of BAFF, APRIL, or other cytokines by the epithelial cells (He et al., 2007; Shang et al., 2008; Xu et al., 2007).

Taken together, the in vivo and in vitro results indicate that direct signaling through TLRs and RARs enhances the production of CXCL13 and BAFF by PP FDCs and contributes to the GC formation and IgA induction in PPs.

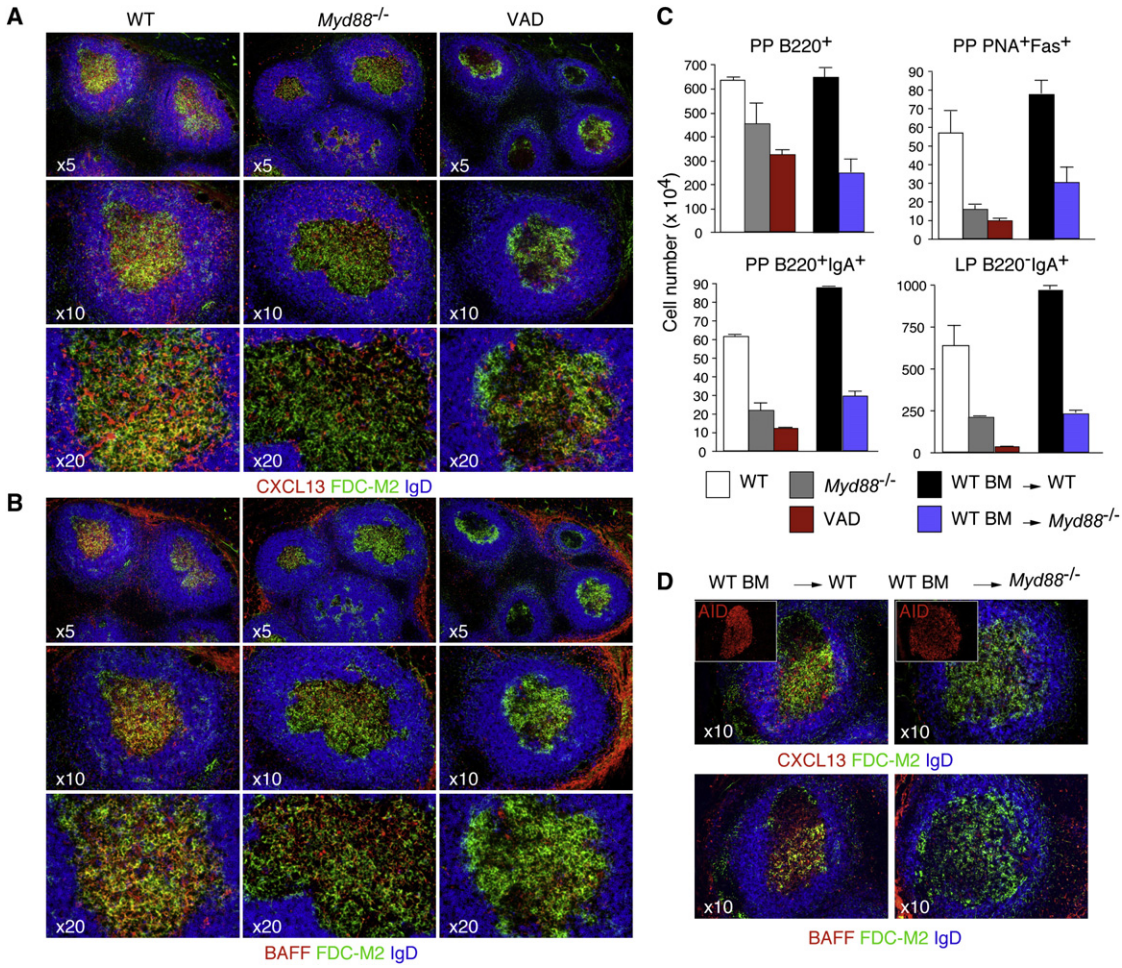

Figure 4. Reduced Expression of CXCL13 and BAFF by PP FDCs and Impaired IgA Generation in *Myd88*$^{-/-}$ and VAD Mice

(A and B) Immunofluorescent microscopy analysis of representative PPs horizontal sections, stained as indicated, from the 2-month-old WT, *Myd88*$^{-/-}$, and VAD mice.

(C) Total numbers of B cells (B220$^+$), GC B cells (B220$^+$PNA$^+$Fas$^+$) and IgA$^+$ B cells (B220$^+$IgA$^+$) from the PPs and IgA plasma cells (B220$^-$IgA$^+$) from the LP of the small intestine of the indicated mice. Means ±SEM for 2–4 mice per group.

(D) Immunofluorescent microscopy analysis of representative PPs horizontal sections, stained as indicated, from WT or *Myd88*$^{-/-}$ mice at 5 weeks after transfer of normal bone marrow cells. AID expression is shown in insets.

PP FDCs Secrete More TGF-β1 Than pLN FDCs

The observations that (1) PP FDCs express high amounts of transcripts for many molecules known to activate TGF-β1 and that (2) several of these transcripts were induced in vitro after stimulation of pLN FDCs with RA and/or Pam2CSK4 prompted us to evaluate the TGF-β1 production by FDCs. The amounts of TGF-β1 transcripts were similar in FDCs isolated from PPs, mLNs, and pLNs and were also comparable between WT, *Myd88*$^{-/-}$, and VAD mice (Figure 5A). Furthermore, the mRNA expression of TGF-β1 remained unchanged after in vitro stimulation of pLN FDCs through TLRs and RARs (Figure 5B).

TGF-β1 production is regulated at transcriptional, posttranscriptional, and posttranslational levels (Annes et al., 2003). Thus, TGF-β1 is produced as a biologically inactive complex composed of mature TGF-β1 homodimer and latency-associated protein (LAP, the amino-terminal propeptide homodimer of the TGF-β1 precursor), and activation of latent TGF-β1 involves, among other events, disruption of the LAP-TGF-β1 complex (Annes et al., 2003). We found that the surface expression of LAP-TGF-β1 was considerably reduced in PP or mLN FDCs isolated from WT mice as compared with PP FDCs from VAD mice (Figure 5C and data not shown). The expression of LAP-TGF-β1 in PP FDCs from *Myd88*$^{-/-}$ mice was reduced compared with VAD mice, yet higher than that in WT mice (Figure 5C). Unlike for PP FDCs, the surface expression of LAP-TGF-β1 on pLN FDCs was comparable between WT, *Myd88*$^{-/-}$, and VAD mice (Figure 5C). These results suggest that stimulation through RARs and TLRs regulates TGF-β1 production by FDCs at the posttranscriptional levels that involve cleavage of the LAP-TGF-β1 complex. In agreement with this, in vitro stimulation of pLN FDCs with RA or Pam2CSK4 and especially the combined stimulation with RA and Pam2CSK4 considerably reduced the surface expression of LAP-TGF-β1 (Figure 5C).

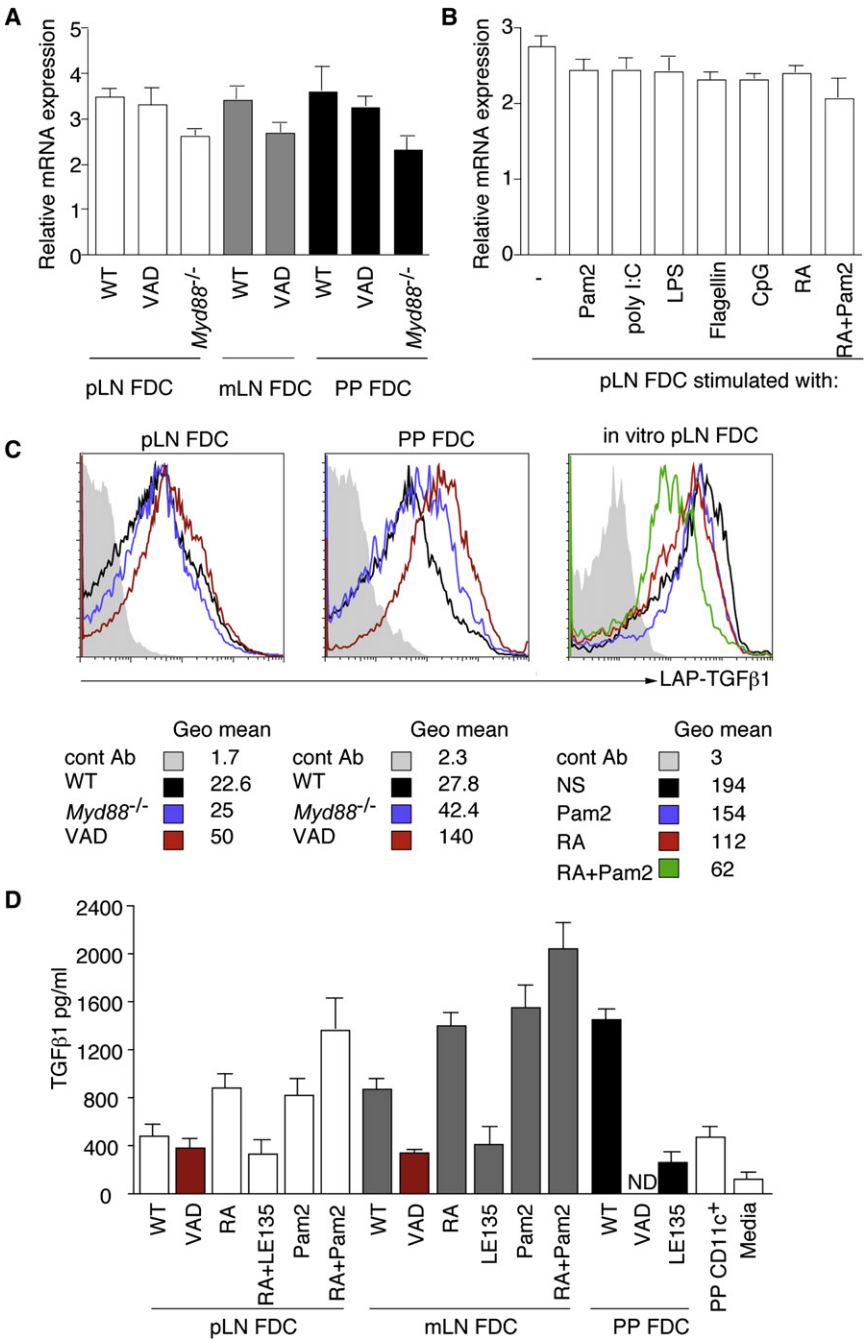

Figure 5. Enhanced TGF-β1 Production by Mucosal FDCs

(A and B) Q-PCR analyses showing expression of *Tgfb1* relative to housekeeping gene *Gapdh* by freshly purified FDCs of the indicated organs and mice (A) and by pLN FDCs isolated from WT mice cultured for 4 days and stimulated as indicated (B) (mean ±SEM).

(C) Overlay histograms of flow cytometry showing LAP-TGF-β1 expression on ex vivo purified FDCs prepared from pLNs or PPs of indicated mice (left and middle panels) and on pLN FDCs cultured 4 days without or with RA, Pam2CSK4, or RA and Pam2CSK4 (right panel). Shaded histograms represent isotype control antibodies. Geometric mean intensities for control and LAP-TGF-β1 antibodies are shown. Data in (A)–(C) are representative of at least three experiments.

(D) Total amount of TGF-β1 in culture supernatants of FDCs prepared from the pLNs, mLNs, and PPs of WT or VAD mice (red bars) cultured as indicated, as determined by ELISA. For comparison, the amount of TGF-β1 in culture supernatants of PP CD11c$^+$ cells and also the culture media is shown. Data are representative of at least three independent experiments (mean ±SEM). ND, not determined.

The amount of secreted TGF-β1 was measured in conditioned media (CM) from 4 day cultures of FDCs isolated from PPs, mLNs, and pLNs. We found that PP FDCs (and mLN FDCs) secreted larger amounts of TGF-β1 than pLN FDCs (Figure 5D). The high secretion of TGF-β1 by mucosal FDCs was largely dependent on stimulation through RARs and TLRs because (1) in vivo deficiency of VA, as well as the addition of RAR antagonists (LE135 or LE540) to the PP FDC or mLN FDC cultures, reduced the amount of TGF-β1 in CM considerably (Figure 5D and data not shown) and (2) stimulation of pLN FDCs (and mLN FDCs) with RA or Pam2SCK4 increased the TGF-β1 production. The concomitant stimulation with RA and Pam2CSK4 had an additive effect on TGF-β1 secretion by FDCs (Figure 5D). Furthermore, PP FDCs and mLN FDCs secreted more TGF-β1 than pLN FDCs even when cultured in VA-depleted media and stimulated with RA at very low concentrations (Figure S5). Thus, PP FDCs and mLN FDCs secrete large amounts of TGF-β1 in response to specific gut stimuli, and that signaling through RARs and TLRs regulates the production of this cytokine by the FDCs through conversion of latent TGF-β1 to active TGF-β1.

Gut FDCs Facilitate Class Switching of Activated B Cells from IgM to IgA

The active form of TGF-β1 produced by FDCs was evaluated by the IgA class-switching assay. To this end, IgA-depleted spleen cells stimulated with LPS and IL-5 were cultured with CM from FDCs isolated from PPs, mLNs, or pLNs. The generation of IgA B cells and IgA plasmablasts was evaluated 5 days later.

Stimulation of splenic cells with LPS and IL-5 in the presence of CM from PP FDCs or CM from mLN FDCs resulted in a very efficient generation of B220$^+$IgA$^+$ B cells and B220$^-$IgA$^+$ plasmablasts (Figure 6A). By contrast, CM from pLN FDCs supported only a very modest switching of activated B cells from IgM to IgA. However, CM from pLN FDCs stimulated with RA and Pam2CSK4 facilitated IgA class switching as

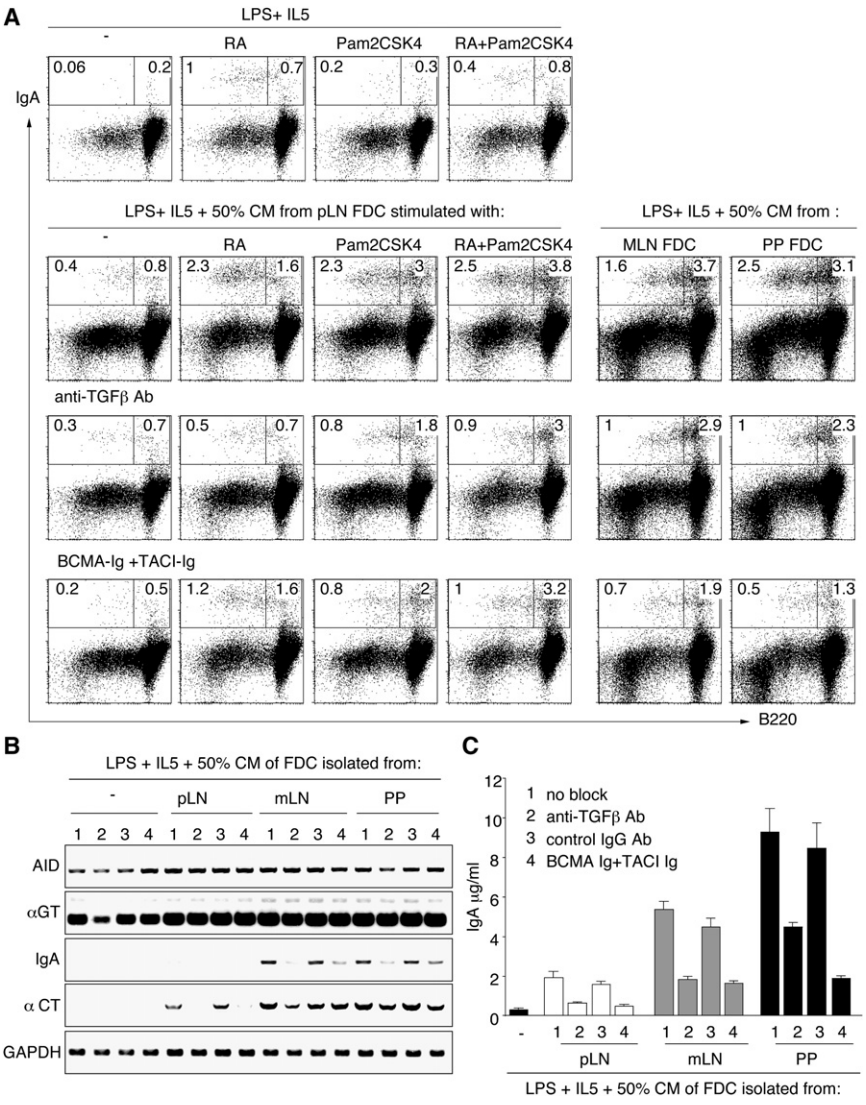

Figure 6. Mucosal FDCs Effectively Support IgA Generation through Secretion of TGF-β1 and BAFF

(A) IgA-depleted spleen cells were cultured for 5 days without (top profiles) and with (left four columns) 50% conditioned media of 4 day culture supernatant of FDCs prepared from pLNs or from mLNs and PPs (right 2 columns) in the presence of stimulants and antibodies, as indicated.

(B) RT-PCR of AID, αGT, IgA (Iμ-Cα), and αCT in IgA-depleted spleen cells cultured 3 days in conditioned media (1), conditioned media with TGF-β antibodies (2) or control antibodies (3), and conditioned media with BCMA-Ig and TACI-Ig (4).

(C) Total amount of secreted IgA in the 5 day supernatants from IgA-depleted spleen cells cultured in conditions indicated in (B). Data are representative of 3–6 independent experiments (mean ±SEM).

efficiently as CM from nonstimulated PP FDCs or mLN FDCs (Figure 6A). This was evidenced at the molecular level (increased germline, postswitched, and circle transcripts for IgA [Kinoshita et al., 2001]) and at the cellular level (increased surface IgA expression as well as the amount of secreted IgAs) (Figures 6A–6C and S6). Notably, stimulation of splenic cells with RA and Pam2CSK4 in the absence of CM induced only minimally the switching of B cells from IgM to IgA (Figure 6A, upper panels).

The enhanced IgA class switching observed with CM from mucosal FDCs as well as TLR- and RA-stimulated pLN FDCs was mostly due to two factors, TGF-β1 and BAFF, because the neutralization of TGF-β1 or the addition of soluble BCMA-Ig and TACI-Ig to these CMs substantially inhibited the IgA^+ B cell generation at molecular and cellular levels (Figures 6A–6C). Thus, PP FDCs conditioned by bacteria and RA contribute to the preferential generation of IgA in PPs through their high secretion of active TGF-β1 and BAFF.

Reduced IgA Synthesis in the Absence of PP FDCs

We further investigated whether the efficiency of IgA generation with CM from various FDCs in vitro is also reflected in vivo. Thus, we compared the frequencies of IgA^+ B cells in GCs from PPs, mLNs, and various pLNs. As shown in Figure S7, the relative efficiency of class switching to IgA was indeed higher in PP and mLN GCs than in endogenous GCs detected in pLNs.

To evaluate more directly the contribution of PP FDCs to IgA generation in gut, we generated FDC-sufficient and FDC-deficient mice by reconstituting *Rag2*$^{-/-}$ mice with BM from WT and lymphotoxin-deficient (*Lta*$^{-/-}$) mice, respectively (Figure 7A). In agreement with previous data (Mebius et al., 1998), mice reconstituted with *Lta*$^{-/-}$ BM failed to develop FDC networks in PPs or mLNs (Figure 7A and data not shown). Even in the absence of FDCs, we could observe many AID-expressing cells within the PP B cell follicles. However, the AID clusters in PPs of *Rag2*$^{-/-}$ mice reconstituted with *Lta*$^{-/-}$ BM differed from those observed in control mice: they were less compact, expressed lower amounts of AID, and were devoid of IgA^+ B cells, yet contained few IgA plasmablasts generated probably with the help of $CD11c^+$ DCs that were found scattered between AID-expressing cells (Litinskiy et al., 2002) (Figure 7A, right panels). Indeed, the frequencies of $B220^+IgA^+$ B cell in PPs and $B220^-IgA^+$ plasma cells in the LP of *Rag2*$^{-/-}$ mice transferred with *Lta*$^{-/-}$ BM were very much lower compared with those in mice reconstituted with WT BM cells (Figures 7A and 7B). The reduced IgA production was not due to intrinsic class switching defect of *Lta*$^{-/-}$ B cells, because in vitro, the efficiency of IgA (or IgG) generation was similar for WT and *Lta* $^{-/-}$ spleen cells (data not shown).Taken together, the results demonstrate that FDCs conditioned by bacteria and RA have a major contribution to IgA synthesis in GCs of PPs.

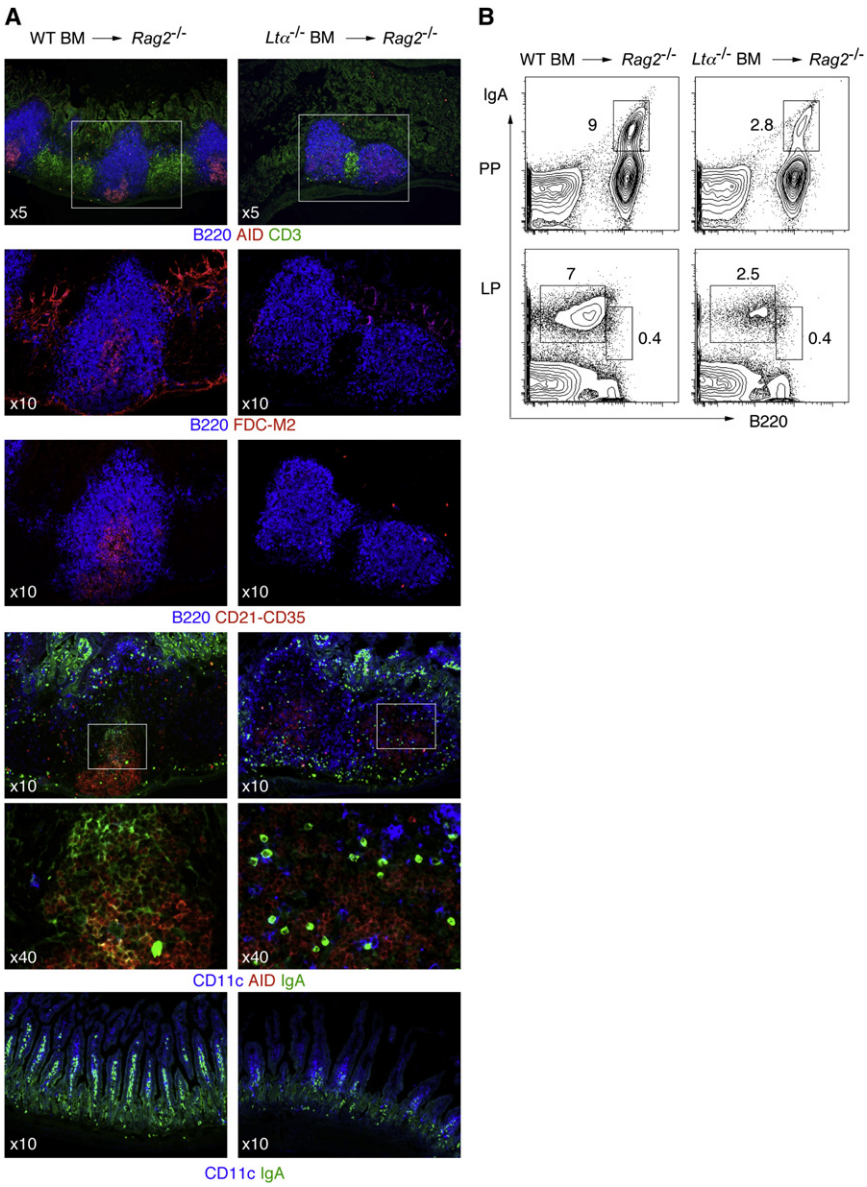

Figure 7. Reduced IgA Generation in PP GCs in the Absence of FDCs

(A) Immunofluorescent microscopy analysis of PP and LP sections, stained as indicated.

(B) Flow cytometric profiles of PP and LP cells from the *Rag2*$^{-/-}$ mice 6 months after reconstitution with bone marrow cells from WT or *Lta*$^{-/-}$ mice. Numbers on plots indicate the frequency of cells in the gate. Data are representative of three experiments.

DISCUSSION

The colonization of gut with commensal bacteria is invariably associated with prompt and abundant generation of gut IgA through multiple pathways. Thus, IgAs can be produced in the absence of any organized follicular structures (Fagarasan et al., 2001; Suzuki et al., 2005; Uematsu et al., 2008) or within scattered small follicular structures called isolated lymphoid follicles (ILFs), with or without T cell help (He et al., 2007; Macpherson et al., 2000; Tsuji et al., 2008). However, the most efficient induction of IgA responses requires PPs and the formation of GCs (Tsuji et al., 2009). Yet surprisingly little is known about the cellular components and molecular mechanisms responsible for IgA synthesis in PP GCs.

In this manuscript, we have revealed that FDCs—cells known to support GC formation—contribute to IgA synthesis in the gut. We demonstrate that FDCs express TLRs and RARs and respond to bacterial and RA stimulation by producing large amounts of chemokines and cytokines required for the recruitment, survival, and functional modulation of lymphocytes in GCs. We propose that, like epithelial cells, FDCs act as sensors, able to perceive signals from the gut environment and to convert these signals into effector molecules for lymphocytes (Rakoff-Nahoum et al., 2004).

TGF-β1 is the major cytokine promoting IgA class switching in PPs, as indicated by the almost complete absence of IgA$^+$ B cells in PPs of mice that lack or have very low expression of TGF-βRII on their B cells (Borsutzky et al., 2004; Cazac and Roes, 2000). We have found that PP FDCs produce large amounts of TGF-β1 and that CM from PP FDCs support very efficiently the generation of IgA$^+$ B cells and IgA plasmablasts. Using three different yet complementary methods by which we measured the surface expression, secretion, and activity of TGF-β1 in functional assays, we have shown that the enhanced production of active TGF-β1 by mucosal FDCs is the result of the continuous and combined stimulation of FDCs through TLRs and RARs.

The mechanisms leading to an enhanced TGF-β1 production by TLR and RAR stimulation of FDCs can be quite complex. For several types of cells (i.e., leukemia cell line, keratinocytes, and endothelial cells), RAR stimulation was reported to increase TGF-β1 expression by enhancing transcription (Batova et al., 1992; Falk et al., 1991). However, in the case of FDCs, we found that RAR and TLR stimulation regulates TGF-β1 production mostly at the posttranscriptional level, by increasing the expression of molecules (ECM, LTBPs, MMPs) involved in the presentation and release of TGF-β1 from the latent LAP-TGF-β1 complex (Annes et al., 2003; Yoshinaga et al., 2008). We still do not know if PP FDCs are the major producers of TGF-β1 in vivo. It is possible that PP FDCs, through their high expression of adhesion molecules and ECM proteins, have an enhanced capacity to capture and retain latent TGF-β1 complex also produced by other cells, such as DCs, ECs, T cells, or B cells

(Suzuki and Fagarasan, 2008). Supporting this idea is the observation that in vivo, the efficiency of IgA generation in GC PPs was higher than that observed in vitro with CM from PP FDCs, yet in the absence of FDCs, the IgA switching was severely impaired.

We have found that mucosal FDCs express "constitutively" high levels of RARβ, and in certain types of cells, elevated RARβ expression was associated with a higher sensitivity to RA (Liu et al., 1996; Teraishi et al., 2003). Indeed, when cultured in VA-depleted media and stimulated with various amounts of RA, mucosal FDCs responded by increasing the TGF-β1 secretion at much lower RA concentrations as compared with pLN FDCs. Furthermore, mLN FDCs prepared from VAD mice, with low RARβ expression, did not respond to RA even at concentrations that were saturating for FDCs isolated from mLN of WT mice. We speculate that the high amounts of RA in the gut contribute not only to increasing the RARβ expression and TGF-β1 production by the gut FDCs, but also to enhancing the sensitivity of gut FDCs to RA.

In addition to TGF-β1, two other cytokines—APRIL and BAFF—contribute to IgA production in gut. Humans expressing mutant TACI molecules and one of the two APRIL-deficient mouse lines exhibit selective IgA deficiency, whereas the overexpression of BAFF results in B cell hyperplasia and a considerable increase in IgA plasma cells in the gut LP (Castigli et al., 2004, 2005; McCarthy et al., 2006; Varfolomeev et al., 2004). Indeed, APRIL secreted by the gut ECs was shown to contribute to IgA production in the LP (He et al., 2007). However, APRIL may have only a minimal effect on IgA production in GCs of PPs, because PP FDCs express low levels of APRIL. In fact, the expression of APRIL in pLN FDCs was higher than in PP FDCs and decreased after in vitro stimulation of pLN FDCs through TLRs (data not shown).

In contrast to APRIL, the expression of BAFF was considerably higher in GC FDCs isolated from PPs as compared with GC FDCs from pLNs. We demonstrate that environmental signals specific to gut, such as LPS and RA, considerably augment the expression of BAFF by mucosal FDCs. A higher production of BAFF by the PP FDCs than the pLN FDCs may be highly relevant for the biology of mucosal GCs, where a large proportion of activated B cells that undergo rapid proliferation or that have just completed class-switch recombination are most susceptible to cell death. Supporting this idea, the frequencies of GC B cells and IgA^+ B cells in PPs of VAD and $Myd88^{-/-}$ mice were very much reduced compared with those in WT mice. Furthermore, when using the in vitro class-switching assay, we found that abrogation of BAFF activity reduced the IgA supportive capacity of CM from PP and mLN FDCs or from pLN FDCs stimulated through TLR and RARs. The block of BAFF had a more dramatic effect on the postswitched IgA transcripts and IgA levels than on the α circle transcripts (αCT), further supporting the idea that BAFF is affecting not so much the IgA class switching per se, but rather the survival and differentiation of recently switched B cells into plasmablasts. Other FDC factors, such as clusterin (Huber et al., 2005), may also contribute to the survival of newly generated IgA^+ B cells, but this remains to be determined in future studies.

Similar to BAFF, the expression of CXCL13 was augmented upon stimulation of FDCs by bacteria and RA. Indeed, MyD88 deficiency in the SC compartment or the VA deficiency caused a severe reduction of CXCL13. The impaired production of CXCL13 and BAFF by FDCs correlated with a marked reduction of B cell and GC B cell numbers in PPs of VAD mice and mice lacking MyD88 in FDCs.

Thus, the augmented expression of TGF-β1 activators, BAFF and CXCL13, by PP FDCs depends on signaling through pathways involving TLR-MyD88, RA, and activation of the NF-κB and RAR transcription factors. Interestingly, several genes like *Tnfsf13b*, *Cxcl13*, and *Mmp9* contain near their promoter regions binding sites for RARs, especially RARβ (van de Pavert et al., 2009) (data not shown). It is possible that RARβ, which is highly expressed by mucosal FDCs, may have a direct effect on transcriptional regulation of "signature genes" expressed by PP FDCs, but this remains to be formally proven in future studies.

In conclusion, FDCs are able to detect and respond to environmental stimuli in the gut, such as microbial and metabolic components. The "adaptation" of FDCs to the presence of gut stimuli involves an enhanced production of molecules that facilitate the recruitment, motility, and survival of cells in GCs. It also involves accelerated dynamics of the ECM components that facilitate the conversion of TGF-β1 from the latent form to the active cytokine, with impact on the IgA generation in gut. Like TGF-β1, IgA is a molecule with known anti-inflammatory properties (Cerutti and Rescigno, 2008; Peterson et al., 2007). Other factors induced by TLR and RA stimulation of FDCs may also act as negative regulators. Indeed, several molecules with tissue-protective, anti-inflammatory, and antitumor properties (i.e., clusterin, metallothionein 2, transgelin, CXCL1) were induced in FDCs by the same stimuli that positively regulate the IgA synthesis. Thus, the elucidation of additional mechanisms employed by this powerful, continuous, and diverse stimulation in the gut will undoubtedly lead to further understanding of how mucosal homeostasis is achieved and allow for manipulation of these mechanisms to prevent excessive activation that causes inflammation, autoimmunity, or tumor formation in the gut.

EXPERIMENTAL PROCEDURES

Mice and Immunizations

All mice were bred and maintained in specific pathogen-free conditions (SPF) at the animal facility of Research Center for Allergy and Immunology, RIKEN (Yokohama, Japan), except DR5-luciferase reporter mice that were bred and analyzed at the Biomedical Center, Lund University (Lund, Sweden). Balb/c WT mice and $Lta^{-/-}$ mice (on C57BL/6 background) were purchased from Charles River Japan and Jackson Laboratory, respectively. $Myd88^{-/-}$ mice and $Rag2^{-/-}$ mice have been described previously (Ha et al., 2006). VAD mice were generated as previously described (Iwata et al., 2004). In brief, pregnant female mice were fed vitamin A-free diet (Oriental Yeast, Tokyo), and pups were maintained on the same diet until the analyses. For immunizations, mice were immunized subcutaneously (foot pad, base of tail, lateral thigh, and base of ears) with 1 mg/ml TNP-keyhole limpet hemocyanin (TNP_{17}-KLH, Biosearch Technologies) in 50% IFA (Wako), 50% CFA (Sigma), and 50% CFA with Pam2CSK4 (2 μg/ml; InvivoGen). Draining LNs (popliteal, inguinal, axillary, brachial, and cervical LNs) were collected at day 7 after immunization. All experiments were performed in accordance with approved protocols from the Institutional Animal Care at RIKEN and from the Lund/Malmö regional ethical committee.

Bone Marrow Transfers

BM cells (1×10^7) from Balb/c WT mice were injected intravenously into 7 Gy irradiated Balb/c WT and $Myd88^{-/-}$ mice. To generate FDC-sufficient and FDC-deficient mice, 1×10^7 BM cells from C57BL/6 or $Lta^{-/-}$ mice were injected intravenously into nonirradiated C57BL/6 $Rag2^{-/-}$ mice. After transfer,

mice were given 500 mg/l ampicillin (Sigma) and 1 g/l neomycin (Sigma) in drinking water for 2 weeks.

Antibodies

The following mAbs were purchased from BD Bioscience: purified FDC-M1, phycoerythrin (PE)-conjugated anti-CD21 or CD35 (7G6), allophycocyanin (APC)-conjugated anti-B220 (RA3-6B2), fluorescein isothiocyanate (FITC)-conjugated anti-CD16 or CD32 (2.4G2), anti-Fas (Jo2), anti-CD21 or CD35 (7G6), anti-IgG1 (A85-1), biotin-conjugated anti-CD3 (500A2), and PE-Cy7-conjugated anti-Fas (Jo2). The following mAbs were purchased from eBioscience: PE-conjugated anti-ICAM-1 (YN1/1.7.4), anti-mouse TLR2 (6C2), anti-mouse TLR4/MD2 (MTS510), anti-mouse TLR4 (UT41), purified or eFluor 450-conjugated anti-IgD (11-26c), biotin or Alexa Fluor 700-conjugated anti-B220 (RA3-6B2), and purified anti-CD11c (N418). Purified anti-IgD was labeled with Alexa Fluor 647 by using Alexa Fluor 647 Monoclonal Antibody Labeling Kit (Molecular Probes). PE-conjugated anti-IgA was from Southern Biotechnology Inc. R-PE-conjugated anti-VCAM-1 (M/K-2) was from CHEMICON International, Inc. Goat anti-LTβR was from GT. Goat anti-CXCL13, biotin-conjugated goat anti-mouse BAFF/TNFSF13b, and PE-conjugated anti-human LAP-TGF-β1 (27232) were from R&D Systems. Biotin-conjugated FDC-M2 was from ImmunoKontact. Biotinylated peanut agglutinin (PNA) was from VECTOR laboratories. APC-streptavidin was from eBioscience. PE-streptavidin was from Molecular Probes. Mouse AID monoclonal antibody (MAID-2) has been previously described (Tsuji et al., 2008).

Cell Preparations

The preparation of FDCs was performed based on the previous report, with minor modifications (Sukumar et al., 2006). Between ten and 20 mice were irradiated (10 Gy) 24 hr before the experiment. Cervical, axillar, brachial, inguinal, and popliteal LNs were pooled as pLNs. mLNs and PPs were collected separately. For pLNs and mLNs, capsules were teased with 26G needles. For PPs, epithelial cells were removed by stirring in PBS containing 1 mM EDTA for 15 min at 37°C, and then PPs were cut into small pieces. Tissues were digested twice for 60 and 30 min with a cocktail of liberase blendzyme 2 (100 μg/ml Roche) and DNase (333 μg/ml Sigma) or with a cocktail of collagenase D (1 mg/ml, Roche), dispase I (0.1 mg/ml, Roche), and DNase I (333 μg/ml, Sigma). Collected cells were incubated with FDC-M1, biotin-conjugated anti-rat κ L chain (MRK1, BD Biosciences), and anti-biotin microbeads (Miltenyi Biotec) and then magnetically enriched. The enriched cells were reincubated with FDC-M1 and CD21 or CD35 antibodies, and then FDC-M1^{hi}CD21-CD35^{+} gated cells were sorted on a FACSAria (Becton Dickinson) using the 100 μm nozzle. For LAP-TGF-β1 staining, cells were washed twice with PBS supplemented with 0.5% BSA and incubated with mouse Fc-block (eBioscience) for 15 min on ice, followed by PE-conjugated anti-human LAP-TGF-β1 or isotype control for 30 min in dark at 4°C.

Cell Cultures

Magnetically purified FDCs (2 × 10^5 cells/well, 96-well plates) were cultured in DMEM with 10% fetal calf serum (FCS), 0.02 M HEPES, 0.2 mM nonessential amino acids (NEAA), TNF-α (5 ng/ml; R&D Systems), and anti-LTβR (1 μg/ml; eBio3C8; eBioscience). Cultured cells did not adhere on the plastic after overnight incubation, but most of them spread out and adhered on the culture plates (IWAKI) at day 3 of culture. Then, nonadherent cells (mostly FDC-M1$^-$ and CD21 or CD35$^-$ contaminating cells) were washed out and adherent cells (usually 1 × 10^4 cells) were further cultured without or with the following stimuli: Pam2CSK4 (100 ng/ml; InvivoGen), Pam3CSK4 (100 ng/ml; InvivoGen), Poly (I:C) (1 μg/ml; Sigma), LPS (20 μg/ml; Sigma), flagellin (100 ng/ml; InvivoGen, from *S. thyphimurium*), CpG (100 nM; ODN1668), all-*trans*-retinoic acid (RA 40 nM; Sigma), LE135 (1 μM; Tocris), LE540 (1 μM; Wako), CD40L (500 ng/ml; PeproTech Inc.), IL-21 (20 ng/ml; R&D Systems), and human TGF-β1 (1 ng/ml; R&D Systems). To remove VA from culture media, FCS was mixed with pure ethanol at 1:4 ratio, and precipitated proteins were collected, dissolved in culture media, filtrated, and then applied for cultures with HEPES, NEAA, TNF-α, and anti-LTβR.

For in vitro IgA class-switching assay, IgA-depleted spleen cells were isolated as described (Fagarasan et al., 2001). IgA-depleted spleen cells were cultured for 5 days in DMEM supplemented with 10% FCS, L-glutamine, sodium pyruvate, HEPES, 2-mercaptoethanol, and 50% CM (from 4 day culture supernatant of FDCs). Cells were stimulated with LPS (20 μg/ml; Sigma) and IL-5 (100 U/ml; R&D Systems) in the presence or absence of BCMA-Ig and TACI-Ig (30 μg/ml), pan-specific anti-TGF-β antibodies (35 μg/ml), or control IgG (35 μg/ml), all from R&D Systems. In some experiments, human TGF-β1 (1 ng/ml; R&D Systems) was used as control for IgA switching.

Flow Cytometry

Flow cytometry analyses were performed on FACSCalibur or FACSAria (BD Biosciences), and data were analyzed using FlowJo software (Tree Star, Inc.) or CellQuest software (BD Biosciences).

Immunohistochemical Analysis

Intestine was washed with PBS after opening or by flushing and then fixed at 4°C in a fresh solution of 4% paraformaldehyde (Wako). The samples were washed in PBS, incubated in a solution of 30% sucrose, embedded in OCT compound (Sakura Finetechnical), and frozen with liquid nitrogen. Frozen blocks were sectioned at 8 μm, dried overnight, and then blocked in TNB buffer (PerkinElmer Life Science) containing 5% normal donkey serum. Endogenous biotin was blocked with the Biotin Blocking Kit (Vector Laboratories), and endogenous peroxidase activity was quenched with 1% H_2O_2. The primary antibodies in TNB buffer were applied for 1.5 hr at room temperature or overnight at 4°C. Slides were washed and incubated with biotin-conjugated secondary antibodies, followed by incubation with streptavidin-HRP conjugate (Zymed Laboratories), and then the antigens were visualized with Tyramide Signal Amplification (TSA) kit (PerkinElmer Life Science) according to the manufacturer's instructions. Slides were washed, incubated with DAPI (Sigma), and mounted with Fluoromount-G (Southern Biotechnology Associates). Slides were examined with a Zeiss Axioplan 2 fluorescence microscope. Automated image analyses were performed with ImageJ as previously described (Tsuji et al., 2008).

ELISA

IgA levels in the culture supernatants were determined by enzyme-linked immunosorbent assay (ELISA). TGF-β1 levels in the culture supernatants were determined with Human/Mouse TGF-β1 ELISA Kit (eBioscience) or TGF-β1E$_{max}$ ImmunoAssay System (Promega).

Gene Expression Profiles

Total RNA was isolated from ex vivo purified or in vitro cultured FDCs using TRIzol Reagent (Invitrogen) or RNeasy Mini Kit (QIAGEN). RNA (100 ng) was subjected to biotinylated cRNA synthesis by using Two-Cycle Target Labeling Kit (Affymetrix) or Ovation RNA Amplification System V2 and hybridized with Mouse Genome 430 2.0 Arrays (Affymetrix). The signal intensities for each probe set were calculated with gcRMA method in a GeneSpring GX 7.3 software package (Agilent). Criteria for the probe selection of genes induced by stimulation with bacterial components or RA were as follows: (1) expressed more (2-fold) in PP FDCs than in pLN FDCs isolated from both from naive and immunized mice; (2) upregulated (3-fold) upon any type of stimulation in vitro. The probes that fulfilled these conditions were selected (249 probes).

For RT-PCR, cDNA was synthesized by using random hexamers after DNase I treatment (DNA-free; Ambion). All procedures were performed according to the manufacturer's instructions (Invitrogen). Quantitative real-time PCR was performed on a LightCycler 480 thermal cycler using SYBR Green Supermix according to instructions and analyzed by software (Roche). All primers were determined by Beacon Designer software (PREMIER Biosoft International).

Luciferase Expression Analysis in FDC from DR5-Luciferase Mice

Total RNA was extracted using RNeasy Micro Kit (QIAGEN) and cDNA synthesized using SuperScript III and a 1:1 mixture of oligo-dT and random hexamers (all from Invitrogen). Quantitative RT-PCR reactions were set up using Maxima SYBR Green qPCR Master Mix (Fermentas) and carried out in Bio-Rad MyiQ Thermal Cycler. Primer sequences were as follows: β-actin forward, 5′-GAGAGGGAAATCGTGCGTGACA-3′; β-actin reverse, 5′- GTTTCATGG ATGCCACAGGAT-3′; Luciferase forward, 5′-CGTTCGTCACATCTCATCTAC CTC-3′; Luciferase reverse: 5′-CCACATATCAAATATCCGAGTGT-3′.

ACCESSION NUMBERS

The microarray data are available in the Gene Expression Omnibus (GEO) database (http://www.ncbi.nlm.nih.gov/gds) under the accession number GSE19401.

SUPPLEMENTAL INFORMATION

Supplemental Information includes seven figures and can be found with this article online at doi:10.1016/j.immuni.2010.07.003.

ACKNOWLEDGMENTS

We thank Y. Doi, A. Yagisawa, and Y. Tsutsui for technical assistance; R. Blomhoff, M. Iwata, and H. Ohmori for sharing reagents with us; and T. Honjo, M. Hikida, T. Katakai, and O. Kanagawa for helpful discussion and for comments on the manuscript. This work is supported in part by a strategic research program grant for R&D to S.F. and by a grant from The Naito Foundation to K. Suzuki.

Received: December 9, 2009
Revised: April 13, 2010
Accepted: May 11, 2010
Published: July 22, 2010

REFERENCES

Allen, C.D., and Cyster, J.G. (2008). Follicular dendritic cell networks of primary follicles and germinal centers: phenotype and function. Semin. Immunol. *20*, 14–25.

Annes, J.P., Munger, J.S., and Rifkin, D.B. (2003). Making sense of latent TGFbeta activation. J. Cell Sci. *116*, 217–224.

Batova, A., Danielpour, D., Pirisi, L., and Creek, K.E. (1992). Retinoic acid induces secretion of latent transforming growth factor beta 1 and beta 2 in normal and human papillomavirus type 16-immortalized human keratinocytes. Cell Growth Differ. *3*, 763–772.

Borsutzky, S., Cazac, B.B., Roes, J., and Guzmán, C.A. (2004). TGF-beta receptor signaling is critical for mucosal IgA responses. J. Immunol. *173*, 3305–3309.

Casola, S., Otipoby, K.L., Alimzhanov, M., Humme, S., Uyttersprot, N., Kutok, J.L., Carroll, M.C., and Rajewsky, K. (2004). B cell receptor signal strength determines B cell fate. Nat. Immunol. *5*, 317–327.

Castigli, E., Scott, S., Dedeoglu, F., Bryce, P., Jabara, H., Bhan, A.K., Mizoguchi, E., and Geha, R.S. (2004). Impaired IgA class switching in APRIL-deficient mice. Proc. Natl. Acad. Sci. USA *101*, 3903–3908.

Castigli, E., Wilson, S.A., Garibyan, L., Rachid, R., Bonilla, F., Schneider, L., and Geha, R.S. (2005). TACI is mutant in common variable immunodeficiency and IgA deficiency. Nat. Genet. *37*, 829–834.

Cazac, B.B., and Roes, J. (2000). TGF-beta receptor controls B cell responsiveness and induction of IgA in vivo. Immunity *13*, 443–451.

Cerutti, A., and Rescigno, M. (2008). The biology of intestinal immunoglobulin A responses. Immunity *28*, 740–750.

El Shikh, M.E., El Sayed, R.M., Wu, Y., Szakal, A.K., and Tew, J.G. (2007). TLR4 on follicular dendritic cells: an activation pathway that promotes accessory activity. J. Immunol. *179*, 4444–4450.

Fagarasan, S., Kinoshita, K., Muramatsu, M., Ikuta, K., and Honjo, T. (2001). In situ class switching and differentiation to IgA-producing cells in the gut lamina propria. Nature *413*, 639–643.

Fagarasan, S., Muramatsu, M., Suzuki, K., Nagaoka, H., Hiai, H., and Honjo, T. (2002). Critical roles of activation-induced cytidine deaminase in the homeostasis of gut flora. Science *298*, 1424–1427.

Falk, L.A., De Benedetti, F., Lohrey, N., Birchenall-Roberts, M.C., Ellingsworth, L.W., Faltynek, C.R., and Ruscetti, F.W. (1991). Induction of transforming growth factor-beta 1 (TGF-beta 1), receptor expression and TGF-beta 1 protein production in retinoic acid-treated HL-60 cells: possible TGF-beta 1-mediated autocrine inhibition. Blood *77*, 1248–1255.

Germain, P., Chambon, P., Eichele, G., Evans, R.M., Lazar, M.A., Leid, M., De Lera, A.R., Lotan, R., Mangelsdorf, D.J., and Gronemeyer, H. (2006). International Union of Pharmacology. LX. Retinoic acid receptors. Pharmacol. Rev. *58*, 712–725.

Gommerman, J.L., and Browning, J.L. (2003). Lymphotoxin/light, lymphoid microenvironments and autoimmune disease. Nat. Rev. Immunol. *3*, 642–655.

Grouard, G., de Bouteiller, O., Banchereau, J., and Liu, Y.J. (1995). Human follicular dendritic cells enhance cytokine-dependent growth and differentiation of CD40-activated B cells. J. Immunol. *155*, 3345–3352.

Ha, S.A., Tsuji, M., Suzuki, K., Meek, B., Yasuda, N., Kaisho, T., and Fagarasan, S. (2006). Regulation of B1 cell migration by signals through Toll-like receptors. J. Exp. Med. *203*, 2541–2550.

He, B., Xu, W., Santini, P.A., Polydorides, A.D., Chiu, A., Estrella, J., Shan, M., Chadburn, A., Villanacci, V., Plebani, A., et al. (2007). Intestinal bacteria trigger T cell-independent immunoglobulin A(2) class switching by inducing epithelial-cell secretion of the cytokine APRIL. Immunity *26*, 812–826.

Huber, C., Thielen, C., Seeger, H., Schwarz, P., Montrasio, F., Wilson, M.R., Heinen, E., Fu, Y.X., Miele, G., and Aguzzi, A. (2005). Lymphotoxin-beta receptor-dependent genes in lymph node and follicular dendritic cell transcriptomes. J. Immunol. *174*, 5526–5536.

Iwata, M., Hirakiyama, A., Eshima, Y., Kagechika, H., Kato, C., and Song, S.Y. (2004). Retinoic acid imprints gut-homing specificity on T cells. Immunity *21*, 527–538.

Katakai, T., Hara, T., Sugai, M., Gonda, H., and Shimizu, A. (2004). Lymph node fibroblastic reticular cells construct the stromal reticulum via contact with lymphocytes. J. Exp. Med. *200*, 783–795.

King, C., Tangye, S.G., and Mackay, C.R. (2008). T follicular helper (TFH) cells in normal and dysregulated immune responses. Annu. Rev. Immunol. *26*, 741–766.

Kinoshita, K., Harigai, M., Fagarasan, S., Muramatsu, M., and Honjo, T. (2001). A hallmark of active class switch recombination: transcripts directed by I promoters on looped-out circular DNAs. Proc. Natl. Acad. Sci. USA *98*, 12620–12623.

Kranich, J., Krautler, N.J., Heinen, E., Polymenidou, M., Bridel, C., Schildknecht, A., Huber, C., Kosco-Vilbois, M.H., Zinkernagel, R., Miele, G., and Aguzzi, A. (2008). Follicular dendritic cells control engulfment of apoptotic bodies by secreting Mfge8. J. Exp. Med. *205*, 1293–1302.

Litinskiy, M.B., Nardelli, B., Hilbert, D.M., He, B., Schaffer, A., Casali, P., and Cerutti, A. (2002). DCs induce CD40-independent immunoglobulin class switching through BLyS and APRIL. Nat. Immunol. *3*, 822–829.

Liu, Y., Lee, M.O., Wang, H.G., Li, Y., Hashimoto, Y., Klaus, M., Reed, J.C., and Zhang, X. (1996). Retinoic acid receptor beta mediates the growth-inhibitory effect of retinoic acid by promoting apoptosis in human breast cancer cells. Mol. Cell. Biol. *16*, 1138–1149.

Liu, P.T., Krutzik, S.R., Kim, J., and Modlin, R.L. (2005). Cutting edge: all-trans retinoic acid down-regulates TLR2 expression and function. J. Immunol. *174*, 2467–2470.

Luther, S.A., Tang, H.L., Hyman, P.L., Farr, A.G., and Cyster, J.G. (2000). Coexpression of the chemokines ELC and SLC by T zone stromal cells and deletion of the ELC gene in the plt/plt mouse. Proc. Natl. Acad. Sci. USA *97*, 12694–12699.

Macpherson, A.J., Gatto, D., Sainsbury, E., Harriman, G.R., Hengartner, H., and Zinkernagel, R.M. (2000). A primitive T cell-independent mechanism of intestinal mucosal IgA responses to commensal bacteria. Science *288*, 2222–2226.

McCarthy, D.D., Chiu, S., Gao, Y., Summers-deLuca, L.E., and Gommerman, J.L. (2006). BAFF induces a hyper-IgA syndrome in the intestinal lamina propria concomitant with IgA deposition in the kidney independent of LIGHT. Cell. Immunol. *241*, 85–94.

Mebius, R.E., van Tuijl, S., Weissman, I.L., and Randall, T.D. (1998). Transfer of primitive stem/progenitor bone marrow cells from LT alpha-/- donors to

wild-type hosts: implications for the generation of architectural events in lymphoid B cell domains. J. Immunol. *161*, 3836–3843.

Muramatsu, M., Kinoshita, K., Fagarasan, S., Yamada, S., Shinkai, Y., and Honjo, T. (2000). Class switch recombination and hypermutation require activation-induced cytidine deaminase (AID), a potential RNA editing enzyme. Cell *102*, 553–563.

Nishikawa, Y., Hikida, M., Magari, M., Kanayama, N., Mori, M., Kitamura, H., Kurosaki, T., and Ohmori, H. (2006). Establishment of lymphotoxin beta receptor signaling-dependent cell lines with follicular dendritic cell phenotypes from mouse lymph nodes. J. Immunol. *177*, 5204–5214.

Nomura, F., Akashi, S., Sakao, Y., Sato, S., Kawai, T., Matsumoto, M., Nakanishi, K., Kimoto, M., Miyake, K., Takeda, K., and Akira, S. (2000). Cutting edge: endotoxin tolerance in mouse peritoneal macrophages correlates with down-regulation of surface toll-like receptor 4 expression. J. Immunol. *164*, 3476–3479.

Peterson, D.A., McNulty, N.P., Guruge, J.L., and Gordon, J.I. (2007). IgA response to symbiotic bacteria as a mediator of gut homeostasis. Cell Host Microbe *2*, 328–339.

Rakoff-Nahoum, S., Paglino, J., Eslami-Varzaneh, F., Edberg, S., and Medzhitov, R. (2004). Recognition of commensal microflora by toll-like receptors is required for intestinal homeostasis. Cell *118*, 229–241.

Shang, L., Fukata, M., Thirunarayanan, N., Martin, A.P., Arnaboldi, P., Maussang, D., Berin, C., Unkeless, J.C., Mayer, L., Abreu, M.T., and Lira, S.A. (2008). Toll-like receptor signaling in small intestinal epithelium promotes B-cell recruitment and IgA production in lamina propria. Gastroenterology *135*, 529–538.

Sukumar, S., Szakal, A.K., and Tew, J.G. (2006). Isolation of functionally active murine follicular dendritic cells. J. Immunol. Methods *313*, 81–95.

Suzuki, K., and Fagarasan, S. (2008). How host-bacterial interactions lead to IgA synthesis in the gut. Trends Immunol. *29*, 523–531.

Suzuki, K., Meek, B., Doi, Y., Muramatsu, M., Chiba, T., Honjo, T., and Fagarasan, S. (2004). Aberrant expansion of segmented filamentous bacteria in IgA-deficient gut. Proc. Natl. Acad. Sci. USA *101*, 1981–1986.

Suzuki, K., Meek, B., Doi, Y., Honjo, T., and Fagarasan, S. (2005). Two distinctive pathways for recruitment of naive and primed IgM+ B cells to the gut lamina propria. Proc. Natl. Acad. Sci. USA *102*, 2482–2486.

Svensson, M., Johansson-Lindbom, B., Zapata, F., Jaensson, E., Austenaa, L.M., Blomhoff, R., and Agace, W.W. (2008). Retinoic acid receptor signaling levels and antigen dose regulate gut homing receptor expression on CD8+ T cells. Mucosal Immunol *1*, 38–48.

Takeda, K., and Akira, S. (2004). TLR signaling pathways. Semin. Immunol. *16*, 3–9.

Teraishi, F., Kadowaki, Y., Tango, Y., Kawashima, T., Umeoka, T., Kagawa, S., Tanaka, N., and Fujiwara, T. (2003). Ectopic p21sdi1 gene transfer induces retinoic acid receptor beta expression and sensitizes human cancer cells to retinoid treatment. Int. J. Cancer *103*, 833–839.

Tsuji, M., Suzuki, K., Kitamura, H., Maruya, M., Kinoshita, K., Ivanov, I.I., Itoh, K., Littman, D.R., and Fagarasan, S. (2008). Requirement for lymphoid tissue-inducer cells in isolated follicle formation and T cell-independent immunoglobulin A generation in the gut. Immunity *29*, 261–271.

Tsuji, M., Komatsu, N., Kawamoto, S., Suzuki, K., Kanagawa, O., Honjo, T., Hori, S., and Fagarasan, S. (2009). Preferential generation of follicular B helper T cells from Foxp3+ T cells in gut Peyer's patches. Science *323*, 1488–1492.

Uematsu, S., Fujimoto, K., Jang, M.H., Yang, B.G., Jung, Y.J., Nishiyama, M., Sato, S., Tsujimura, T., Yamamoto, M., Yokota, Y., et al. (2008). Regulation of humoral and cellular gut immunity by lamina propria dendritic cells expressing Toll-like receptor 5. Nat. Immunol. *9*, 769–776.

van de Pavert, S.A., Olivier, B.J., Goverse, G., Vondenhoff, M.F., Greuter, M., Beke, P., Kusser, K., Höpken, U.E., Lipp, M., Niederreither, K., et al. (2009). Chemokine CXCL13 is essential for lymph node initiation and is induced by retinoic acid and neuronal stimulation. Nat. Immunol. *10*, 1193–1199.

Varfolomeev, E., Kischkel, F., Martin, F., Seshasayee, D., Wang, H., Lawrence, D., Olsson, C., Tom, L., Erickson, S., French, D., et al. (2004). APRIL-deficient mice have normal immune system development. Mol. Cell. Biol. *24*, 997–1006.

Wu, Y., Sukumar, S., El Shikh, M.E., Best, A.M., Szakal, A.K., and Tew, J.G. (2008). Immune complex-bearing follicular dendritic cells deliver a late antigenic signal that promotes somatic hypermutation. J. Immunol. *180*, 281–290.

Xu, W., He, B., Chiu, A., Chadburn, A., Shan, M., Buldys, M., Ding, A., Knowles, D.M., Santini, P.A., and Cerutti, A. (2007). Epithelial cells trigger frontline immunoglobulin class switching through a pathway regulated by the inhibitor SLPI. Nat. Immunol. *8*, 294–303.

Yoshinaga, K., Obata, H., Jurukovski, V., Mazzieri, R., Chen, Y., Zilberberg, L., Huso, D., Melamed, J., Prijatelj, P., Todorovic, V., et al. (2008). Perturbation of transforming growth factor (TGF)-beta1 association with latent TGF-beta binding protein yields inflammation and tumors. Proc. Natl. Acad. Sci. USA *105*, 18758–18763.